

Wigner crystal versus Fermionization for one-dimensional Hubbard models with and without long-range interactions

Zhihao Xu,¹ Linhu Li,¹ Gao Xianlong,² and Shu Chen^{1,*}

¹*Beijing National Laboratory for Condensed Matter Physics,
Institute of Physics, Chinese Academy of Sciences, Beijing 100190, China*

²*Department of Physics, Zhejiang Normal University, Jinhua, Zhejiang Province, 321004, China*
(Dated: July 31, 2012)

The ground state properties of Hubbard model with or without long-range interactions in the regime with strongly repulsive on-site interaction are investigated by means of the exact diagonalization method. We show that the appearance of N -crests in the density profile of a trapped N -fermion system is a natural result of “fermionization” between antiparallel-spin fermions in the strongly repulsive limit and can not be taken as the only signature of Wigner crystal phase, as the static structure factor does not show any signature of crystallization. On the contrary, both the density distribution and static structure factor of Hubbard model with strong long-range interactions display clear signature of Wigner crystal. Our results indicate the important role of long-range interaction in the formation of Wigner crystal.

PACS numbers: 03.75.Ss, 67.85.Lm, 71.10.Fd

I. INTRODUCTION

The Hubbard model has been widely used as a minimal model to describe strongly interacting electrons in a solid and played a particularly important role in understanding the physics related to the quantum magnetism and high-temperature superconductivity. Recent experiment progress in trapping the quantum gas in optical lattice [1–3] has renewed the interest in this basic model [4, 5]. In comparison with real materials in solid, the fermionic quantum gas trapped in optical lattice is a more ideal realization of the Hubbard model [2], which provides a laboratory to simulate and study this basic quantum many-body system from different aspects. Particularly current experiment techniques also prompt intensive study of quantum many-body systems in reduced one-dimensional (1D) systems, among which important benchmarks include experimental realization of the Tonks-Girardeau (TG) gases [6, 7], and the Mott transition in 1D tight tubes [8]. Furthermore, the recent experimental realization of two-component Fermi gases in a quasi-1D geometry with tunable interaction strengths by Feshbach resonance [9] provides a unique possibility to experimentally study the 1D Hubbard model even in the strong interaction limit. The good tunability of optical lattices enables us to experimentally elucidate the subtleties of 1D quantum many-body systems, for example, the physical properties in the strongly interacting limit. Due to recent experimental progress on chromium atoms [10, 11] and heteronuclear polar molecule produced by stimulated Raman adiabatic passage technique [12, 13], dipolar atomic systems with strong long-range dipole-dipole interaction (DDI) have also attracted intensive studies [14–19]. In addition, schemes of creating Coulomb-like interaction

in cold atom systems have also been proposed [20, 21].

In the presence of long-range repulsive interaction, an interesting issue for the 1D fermionic system is the existence of Wigner crystal phase [22]. For a 1D gas of electrons with long-range Coulomb interaction which has been investigated by Schulz in the scheme of bosonization [22], the extremely slow decay of density correlations at wave vector $4k_F$ has been used as a signature of appearance of Wigner crystal. Here $k_F = \pi n$ is the Fermi wave vector with n the particle density. After that, exploring Wigner crystal phase in the short-range interacting fermion systems, for example the Hubbard model, has also been carried out [23–26]. By using bosonization and density matrix renormalization group methods to study the one-dimensional finite Hubbard chains with hard-wall boundaries, a crossover from $2k_F$ - to $4k_F$ -density oscillations with the increasing of repulsion has been found [23, 24], and sometimes the $4k_F$ density oscillations was taken as a signature of the emergency of Wigner crystal. In the limit of infinitely strong interaction, the on-site repulsion imposes an effective Pauli principle between fermions with different spins. Consequently, the ground state in the strong repulsion limit is degenerate for states with different spin configuration [27–29], and thus the ground state density distribution of an equally mixed trapped system is identical to the fully polarized system with the appearance of the doubling of the crests in density profiles. Such a phenomenon, which is also refereed as fermionization, was recently observed by the experiment in a two-particle system with tunable interaction using two fermionic ^6Li atoms [30].

As the density distribution is not solely a convincing criteria of Wigner crystal, the density-density correlation function plays an important role in characterizing the Wigner crystal phase [31]. In the present work, we shall study both the density distribution and density correlation function of the Hubbard model either without or with long-range interactions. For the Hubbard model

*Electronic address: schen@aphy.iphy.ac.cn

with only the short-range interaction, we find that the density correlation function does not show any signature of Wigner-crystal correlations in spite of the fact that the ground-state density profile displays pronounced $4k_F$ Wigner oscillations in the strong repulsion limit. To unveil the role of the interaction range, we then study the Hubbard model with additional long-range interactions and compare the calculated results with those of the Hubbard model. We find that the system with long-range interactions indeed exhibits quite different behaviors from those of short-range Hubbard model. Particularly, the clear evidence in static structure factor has indicated the important role of the long-range interaction in the formation of Wigner crystal.

The remain of the paper is organized as follows. In Sec.II, we introduce our studied models and main conclusions based on the calculation of models. In Sec.III, we present our calculation results of density distributions and static structure factors in subsection A and B for the Hubbard model and Hubbard model with additional long-range interactions, respectively. A summary is given in the last section.

II. MODEL HAMILTONIAN

The basic model describing the short-range interacting fermions in a 1D lattice is the Hubbard model [32]

$$H = -t \sum_{i\sigma} (\hat{c}_{i\sigma}^\dagger \hat{c}_{i+1\sigma} + \text{H.c.}) + U \sum_i \hat{n}_{i\uparrow} \hat{n}_{i\downarrow}, \quad (1)$$

where $\hat{c}_{i\sigma}^\dagger$ (\hat{c}_i) is the creation(annihilation) operator of the fermion with the spin σ , $\hat{n}_{i\uparrow}$ ($\hat{n}_{i\downarrow}$) is the spin-up(down) particle number operator, t is the hopping strength which is set to the unit, and U is the on-site interaction strength. The 1D Hubbard model can be realized by trapping a two-component Fermi gas in a deep 1D optical lattice.

To study the long-range interaction, we consider the following Hamiltonian

$$H = -t \sum_{i\sigma} (\hat{c}_{i\sigma}^\dagger \hat{c}_{i+1\sigma} + \text{H.c.}) + U \sum_i \hat{n}_{i\uparrow} \hat{n}_{i\downarrow} + \frac{1}{2} V \sum_{i \neq j} \frac{\hat{n}_i \hat{n}_j}{|i - j|^\alpha}, \quad (2)$$

with V the strength of the long-range interaction and α the decaying exponent. For dipolar atoms confined in a 1D optical lattices, the dipole-dipole interaction decays as $1/|i - j|^3$ with the exponent $\alpha = 3$ [19], whereas $\alpha = 1$ corresponds to the electron system with long-range Coulomb interaction. In the present work, we consider the case with repulsive on-site interaction $U > 0$ and repulsive long-range interaction $V > 0$.

In the following section, we shall first calculate the density distribution and the density-density correlation

function for the Hubbard model (1) with the on-site interaction strength varying from weak to strong repulsion limit by exact diagonalization method. In order to see the oscillation of the density profile, we shall use open boundary condition (OBC) in the calculation of density distribution, whereas periodic boundary condition (PBC) shall be used in the calculation of structure factor. In the limit of $U \rightarrow \infty$, the total ground-state density distribution with different spin configurations is identical to that of the polarized noninteracting fermions, despite the fact that the spin-dependent densities are different. This is consistent with the exact result obtained via the exact construction of many-body wavefunction [29]. Our numerical diagonalization results also show that the structure factor, which is the Fourier transformation of density-density correlation function, in the infinite repulsion limit also displays the same behavior as the fully polarized fermions. These results suggest that the appearance of the doubling of peaks of the equally mixing system (or $4k_F$ Wigner oscillation) in the infinite repulsion limit can not be taken as a hallmark of the emergency of Wigner crystal. It is just a kind of “fermionization” between fermions with different spins as a result of the effective Pauli principle imposed by the infinite repulsion.

The absence of Wigner crystal phase in the short-range Hubbard model implies that the long-range interaction may play a very important role in the formation of Wigner crystal phase. To unveil its role, we then calculate the density distribution and the density-density correlation function for the Hubbard model with the additional long-range interaction described by Hamiltonian (2). For conveniences, we shall focus our calculation to the case with $\alpha = 1$ for which the long-range interaction decays more slowly than the dipole-dipole interaction. Keeping the on-site interaction fixed, we find that the Wigner crystal phase emerges with the increase of the long-range interaction strength V . Finally, we also calculate the case with $\alpha = 3$ which exhibits similar behavior as the case of $\alpha = 1$.

III. RESULTS AND DISCUSSIONS

A. Fermi-Hubbard model

We first calculate the ground state density distribution $n_i = n_{i\uparrow} + n_{i\downarrow}$ of the Fermi-Hubbard model (1) under the OBC, where $n_{i\sigma} = \langle \hat{n}_{i\sigma} \rangle$ is the spin-dependent ground state density distribution. In Fig.1, we show the density profiles n_i and $n_{i\sigma}$ versus different U for the balanced Fermi-Hubbard model (1) with $N_\uparrow = N_\downarrow = 3$ and the lattice size $L = 24$. For the balanced case, we always have $n_{i\uparrow} = n_{i\downarrow} = n_i/2$. In the limit of $U \rightarrow 0$, we have $n_{i\sigma} = \sum_l^{N_\sigma} |\phi_l|^2$, where $\phi_l(i) = \sqrt{\frac{2}{L+1}} \sin(l \frac{\pi}{L+1} i)$ is the l -th single particle wave function of the open tight binding chain [33], which fulfills the OBC of $\phi_l(0) = \phi_l(L+1) = 0$.

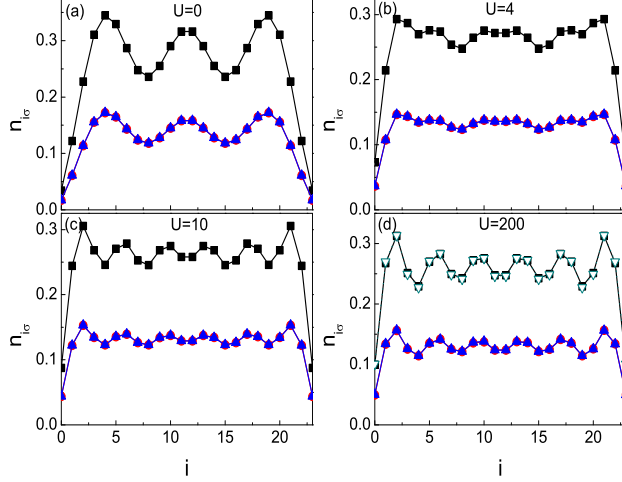


FIG. 1: (Color online) The ground-state density distribution of the Fermi-Hubbard model for different U with $N_\uparrow = N_\downarrow = 3$ confined in a lattice with $L = 24$ under the open boundary condition. Here, solid square is for $n_i = n_{i\uparrow} + n_{i\downarrow}$, solid circle is for $n_{i\uparrow}$ and solid triangle is for $n_{i\downarrow}$. The density distribution n_i in the limit of $U \rightarrow \infty$ is shown in (d) marked by hollow inverted triangles.

It is obvious that there are three crests in the density distribution of n_i for $N_\uparrow = N_\downarrow = 3$ in the weakly interacting limit. As the interaction strength U keeps increasing, the density distribution displays clearly six crests for $U = 10$. In the limit of $U \rightarrow \infty$, we have $n_i = \sum_l^N |\phi_l(i)|^2$ with $N = N_\uparrow + N_\downarrow$ for different spin configurations according to exact construction of many-body wavefunctions [29] due to the induced Pauli exclusion principle between antiparallel spins. As shown in Fig.1, the total density profile for $U = 200$ obtained by the exact diagonalization method is completely overlapped with the exact result in the strongly interacting limit. For the imbalanced case with $N_\uparrow = 2$, $N_\downarrow = 4$ and $L = 24$, we show the change of density profiles of the Hubbard model with the increase of U in Fig.2. Despite the fact that now we have $n_{i\uparrow} \neq n_{i\downarrow}$, the total density distribution also displays clearly six crests for $U = 10$. Also, the total density profile for $U = 200$ coincides with the density profile of the fully polarized system. Our numerical results clearly show that the total density distributions of the interacting fermion systems with different spin configurations are identical in the limit of infinite repulsion [29].

Next we calculate the static structure factor, which is defined as the Fourier transformation of the density-density correlation function:

$$S(k) = \frac{1}{L} \sum_{i,j} e^{ik(i-j)} [\langle \hat{n}_i \hat{n}_j \rangle - \langle \hat{n}_i \rangle \langle \hat{n}_j \rangle], \quad (3)$$

where $k = 2m\pi/L$ with $m = 0, 1, \dots, L$. In general, the

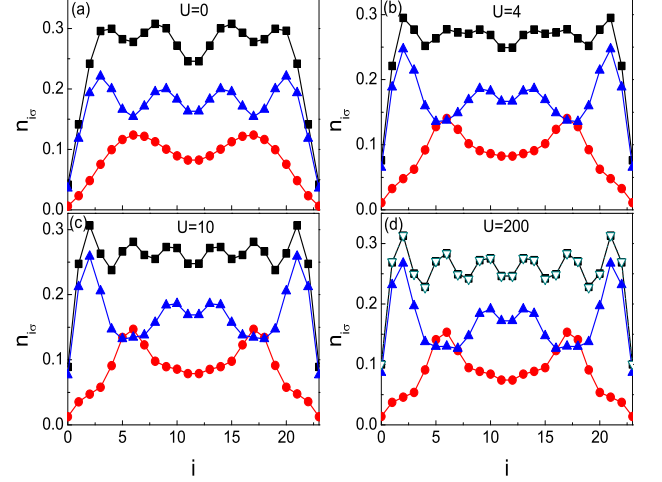


FIG. 2: (Color online) The density distribution of the Hubbard model for different U with $N_\uparrow = 2$, $N_\downarrow = 4$ confined in a lattice with $L = 24$ under the open boundary condition. Here, square is for n_i , circle is for $n_{i\uparrow}$ and triangle is for $n_{i\downarrow}$. The density n_i for $U \rightarrow \infty$ is shown in (d) marked by hollow inverted triangles.

Wigner crystal phase can be characterized by the enhancement of $4k_F$ peak in the static structure factor. In Fig.3(a), we show the change of the static structure factor with the increase of interaction strength U for the case of $N_\uparrow = N_\downarrow = 3$ and $L = 24$ under the PBC. The imbalanced case of $N_\uparrow = 2$ and $N_\downarrow = 4$ is shown in Fig.3(b). For both cases, as U is large enough (for example, $U = 200$), the distribution of the static structure factor approaches to the distribution function of a fully polarized N -particle free fermion system as shown in Fig.3(c). Except of the drops at $kL/(2\pi) = N, L - N$, no obvious peaks in the static structure factor are detected. Our numerical results clearly indicate that the appearance of N peaks in the ground state density profile of a finite trapped Hubbard system is not a mark of the emergence of Wigner crystal in the strongly repulsive limit.

B. Hubbard model with long-range interaction

Now we study the Hamiltonian of the Hubbard model with long-range interaction (2). For the case of $V = 0$, the ground state properties of the system almost does not change with the increase of on-site interaction strength when the U is large enough. In order to explore the effect of the long-range interaction, we shall keep U fixed by taking $U = 200$ and change V in the following calculation. For simplicity, we focus our discussion on the case of $\alpha = 1$, and finally discuss the case of $\alpha = 3$ briefly.

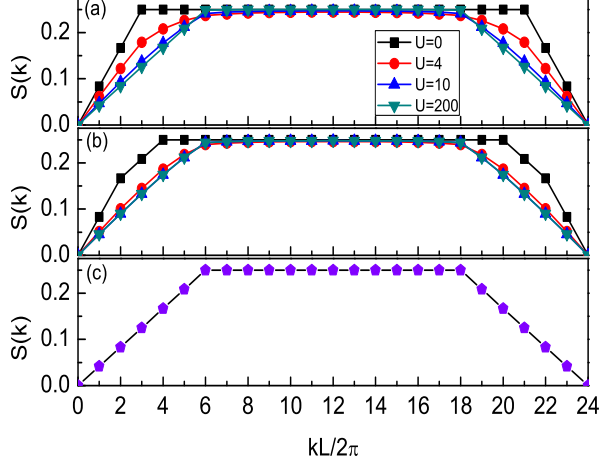


FIG. 3: (Color online) Static structure factor $S(k)$ vs $kL/(2\pi)$ for different U with the periodic boundary condition. (a) is for $N_{\uparrow} = N_{\downarrow} = 3, L = 24$, (b) is the case of $N_{\uparrow} = 2, N_{\downarrow} = 4, L = 24$, and (c) is the case of polarized free fermion system with $N = 6$ and $L = 24$.

In Fig.4, we show the density distribution for the long-range Hubbard model with $\alpha = 1$, $N_{\uparrow} = N_{\downarrow} = 3$ and $L = 24$ under the OBC. At $V = 0$, six crests have already appeared for $U = 200$. Nevertheless, with the increase of V , the particles moves apart away from each other as far as possible to minimizing the total energy. As shown in the Fig.4, very sharp peaks have emerged for $V = 50$ and the height of peaks increases with the increase of V . In contrast to the case of $V = 0$ with only small oscillations, the density profile of the system with a large V resembles six well-separated localized wave packets which distribute uniformly.

To characterize the Wigner crystal phase, we further calculate the static structure factor of the system with $L = 24$, $N_{\uparrow} = N_{\downarrow} = 3$ under the PBC. As shown in Fig.5(a), obvious peaks have already emerged at $kL/(2\pi) = N, L - N$ for $V = 5$. As V keeps increasing, the height of peaks increases further and new peak emerges at $kL/(2\pi) = 2N$. In Fig.5(b), we calculate the static structure factor for a system with $L = 32$, $N_{\uparrow} = 1, N_{\downarrow} = 3$ under the PBC. Similarly, as the long-range interaction keeps increasing, a series of peaks emerge at $kL/(2\pi) = mN$ with m the integer. We also demonstrate data for the static structure factor $S(k)$ versus $k/(n\pi)$ in Fig.6 for systems with $L = 24$, $U = 200$, $V = 150$ and $N = 2, 3, 4, 5, 6$, where $n = N/L$ is filling factor of the system. As shown in Fig.6, systems with different filling factors display similar behaviors in the regime with strong long-range repulsive interaction, i.e., peaks emerging at $k/(n\pi) = 2m$. For the different systems, the positions of the peaks only depend on the

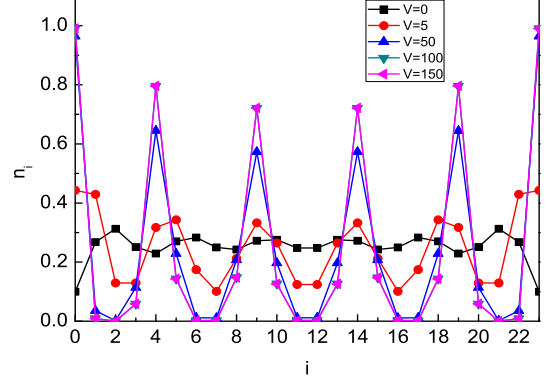


FIG. 4: (Color online) The density distribution of Hubbard model with long-range Coulomb interaction for different V with $U = 200$, $N_{\uparrow} = N_{\downarrow} = 3$, and $L = 24$ under the open boundary condition.

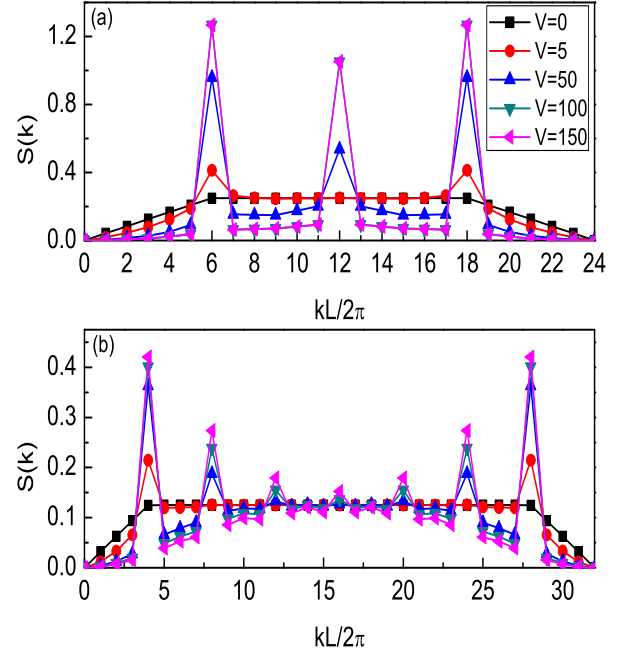


FIG. 5: (Color online) Static structure factor $S(k)$ vs $kL/(2\pi)$ for systems with $U = 200$ and different V under the periodic boundary condition. (a) is for $L = 24$, $N_{\uparrow} = N_{\downarrow} = 3$. (b) is for $L = 32$, $N_{\uparrow} = 1, N_{\downarrow} = 3$.

density n .

Next we consider the Hubbard model with long-range dipole-dipole interactions described by the Hamiltonian of Eq.2 with $\alpha = 3$. In Fig.7(a), we plot the density profiles of the Hubbard model with dipole-dipole interactions for a lattice system with $L = 24$, $N_{\uparrow} = N_{\downarrow} = 3$ under OBC. The static structure factors of the same system with PBC are plotted in Fig.7(b). It is obvious that

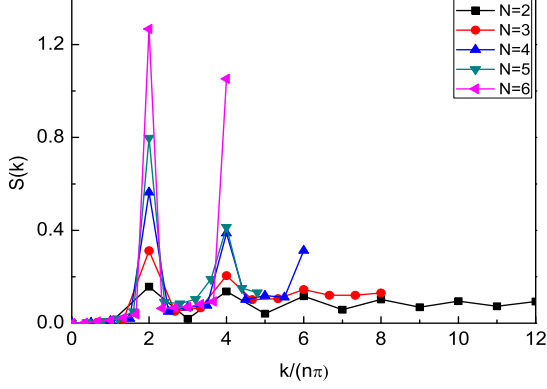


FIG. 6: (Color online) Static structure factor $S(k)$ vs $k/(n\pi)$ ($n = N/L$) for systems with $U = 200$, $V = 150$, $L = 24$ and different N under the periodic boundary condition.

both the density profiles and static structure factors display very similar behaviors as these of the system with $\alpha = 1$. A quantitative difference is that the height of peaks in Fig.7(a) and (b) is lower than that of the corresponding system with Coulomb interaction shown in Fig.4 and Fig.5(a), as the long-range dipole-dipole interaction decays much faster than the Coulomb interaction. Despite the minor differences, our calculated results indicate the existence of the Wigner crystal phase for the Hubbard model with strong dipole-dipole interactions.

As a comparison, we also study the extended Hubbard model described by

$$H = -t \sum_{i\sigma} (\hat{c}_{i\sigma}^\dagger \hat{c}_{i+1\sigma} + \text{H.c.}) + U \sum_i \hat{n}_{i\uparrow} \hat{n}_{i\downarrow} + V \sum_i \hat{n}_i \hat{n}_{i+1}, \quad (4)$$

where only the nearest neighbor short-range interaction is considered. Density profiles and static structure factors of the extended Hubbard model with $L = 24$, $N_\uparrow = N_\downarrow = 3$ are shown in Fig.7(c) and (d), respectively. For $V = 50$, we observe that the oscillations in the density distribution of the extended Hubbard model are enhanced, but the wave packets are still overlapping, which is quite different from the density profile of the dipolar system with well-separated localized wave-packets. With further increasing the nearest neighbor interaction, no obvious change is found. The static structure factors also exhibit different behaviors from the long-range interacting system. As shown in Fig.7(d), only small peaks emerge at $kL/2(\pi) = N, L - N$ for $V = 50$ and the height of peaks does not change obviously with further increasing V . The absence of peaks at $kL/(2\pi) = 2N$ implies that the crystal phase is not detectable. The different behaviors exhibited in systems with the short-range and long-range interactions indicate the important role of the long-range interaction in the formation of Wigner crystal phase.

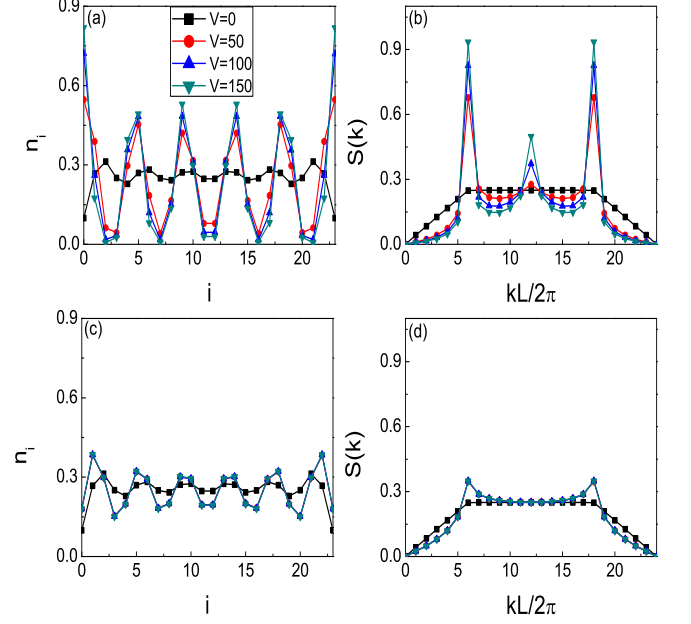


FIG. 7: (Color online) (a) Density profile of the Hubbard model with dipole-dipole interaction under the open boundary condition; (b) static structure factor of the Hubbard model with dipole-dipole interaction under the periodic boundary condition. (c) density profile of the extended Hubbard model with open boundary condition; (d) static structure factor of the extended Hubbard model with periodic boundary condition; Here, $U = 200$, $L = 24$, $N_\uparrow = N_\downarrow = 3$.

IV. SUMMARY

In summary, we study the ground state properties of finite Hubbard systems either with or without long-range interactions by using the exact diagonalization method. We find that the appearance of N -crests in the density profile of Hubbard model in the strongly repulsive limit can not be taken as the only signature of Wigner crystal phase, as it is induced by the effective Pauli principle between antiparallel-spin fermions enforced by the infinite repulsion. The absence of Wigner crystal phase is clearly verified by the calculation of the static structure factor, which shows the same behavior as the polarized free fermion system with no $4k_F$ peaks. If the long-range interaction is considered, the Hubbard model with long-range interaction can form a perfect crystalline phase in the regime with strong long-range repulsions. The existence of the Wigner crystal phase can be well characterized by its density distribution and the emergence of a series of peaks in the static structure factor. Our study unveils the important roles of the long-range interactions in the formation of the Wigner crystal phase. In view of the rapid progress in manipulating the dipolar atomic systems with tunable interactions, our results are possible to be tested by the potential cold atom experiments.

Acknowledgments

This work has been supported by National Program for Basic Research of MOST, NSF of China under Grants

No.11121063, No.11174360 and No.10974234, and 973 grant.

-
- [1] M. Greiner, O. Mandel, T. Esslinger, T. W. Hänsch, and I. Bloch, *Nature (London)* **415**, 39 (2002).
 - [2] R. Jördens, N. Strohmaier, K. Günter, H. Moritz and T. Esslinger, *Nature (London)* **455**, 204-207 (2008).
 - [3] M. Köhl, H. Moritz, T. Stöferle, K. Günter, and T. Esslinger, *Phys. Rev. Lett.* **94**, 080403 (2005).
 - [4] D. Jaksch, C. Bruder, J. I. Cirac, C. W. Gardiner, and P. Zoller, *Phys. Rev. Lett.* **81**, 3108 (1998).
 - [5] W. Hofstetter, J. I. Cirac, P. Zoller, E. Demler, and M. D. Lukin, *Phys. Rev. Lett.* **89**, 220407 (2002).
 - [6] B. Paredes, A. Widera, V. Murg, O. Mandel, S. Fölling, I. Cirac, G. V. Shlyapnikov, T. W. Hänsch, and I. Bloch, *Nature* **429**, 277 (2004).
 - [7] T. Kinoshita, T. Wenger and D. S. Weiss, *Science* **305**, 1125 (2004).
 - [8] T. Stöferle, H. Moritz, C. Schori, M. Köhl, and T. Esslinger, *Phys. Rev. Lett.* **92**, 130404 (2004).
 - [9] H. Moritz, T. Stöferle, K. Günter, M. Köhl, and T. Esslinger, *Phys. Rev. Lett.* **94**, 210401 (2005).
 - [10] T. Lahaye, T. Koch, B. Frölich, M. Fattori, J. Metz, A. Griesmaier, S. Giovanazzi, and T. Pfau, *Nature* **448**, 672 (2007).
 - [11] J. Stuhler, A. Griesmaier, T. Koch, M. Fattori, T. Pfau, S. Giovanazzi, P. Pedri, and L. Santos, *Phys. Rev. Lett.* **95**, 150406 (2005).
 - [12] K.-K. Ni, S. Ospelkaus, M. H. G. de Miranda, A. Pe'er, B. Neyenhuis, J. J. Zirbel, S. Kotochigova, P. S. Julienne, D. S. Jin, and J. Ye, *Science* **322**, 231 (2008).
 - [13] S. Ospelkaus, K.-K. Ni, M. H. G. de Miranda, B. Neyenhuis, D. Wang, S. Kotochigova, P. S. Julienne, D. S. Jin and J. Ye, *Faraday Discuss.* **142**, 351 (2009).
 - [14] S. Yi and L. You, *Phys. Rev. A* **61**, 041604(R) (2000); *Phys. Rev. A* **63**, 053607 (2001).
 - [15] L. Santos, G.V. Shlyapnikov, P. Zoller, and M. Lewenstein, *Phys. Rev. Lett.* **85**, 1791 (2000).
 - [16] M. Dalmonte, G. Pupillo, and P. Zoller, *Phys. Rev. Lett.* **105**, 140401 (2010).
 - [17] R. Citro E. Orignac, S. De Palo, and M. L. Chiofalo, *Phys. Rev. A* **75**, 051602(R) (2007); S. Sinha and L. Santos, *Phys. Rev. Lett.* **99**, 140406 (2007); A. S. Arkhipov, G. E. Astrakharchik, A. V. Belikov, and Y. E. Lozovik, *JETP Lett.* **82**, 39 (2005).
 - [18] F. Deurezbacher, J. C. Cremon, and S. M. Reimann, *Phys. Rev. A* **81**, 063616 (2010); S. Zöllner, G. M. Bruun, C. J. Pethick, and S. M. Reimann, *Phys. Rev. Lett.* **107**, 035301 (2011).
 - [19] Z. H. Xu and S. Chen, *Phys. Rev. A*, **85**, 033606 (2012).
 - [20] D. O'Dell, S. Giovanazzi, G. Kurizki, and V. M. Akulin, *Phys. Rev. Lett.* **84**, 5687 (2000).
 - [21] M. Chalony, J. Barre, B. Marcos, A. Olivetti, and D. Wilkowski, *arXiv:1202.1258*.
 - [22] H. J. Schulz, *Phys. Rev. Lett.* **71**, 1864 (1993).
 - [23] D. Vieira, H. J. P. Freire, V. L. Campo, Jr., and K. Capelle, *J. Magn. Magn. Mater.* **320**, e418 (2008); D. Vieira, *arXiv:1206.5165*.
 - [24] S. A. Söfing, M. Bortz, I. Schneider, A. Struck, M. Fleischhauer, and S. Eggert, *Phys. Rev. B* **79**, 195114 (2009).
 - [25] S. A. Söfing, M. Bortz, and S. Eggert, *Phys. Rev. A* **84**, 021602(R) (2011).
 - [26] S. H. Abedinpour, M. Polini, G. Xianlong, and M. P. Tosi, *Phys. Rev. A* **75**, 015602 (2007).
 - [27] M. Ogata and H. Shiba, *Phys. Rev. B* **41**, 2326 (1990).
 - [28] M. D. Girardeau and A. Minguzzi, *Phys. Rev. Lett.* **99**, 230402 (2007).
 - [29] L. Guan, S. Chen, Y. Wang, and Z.-Q. Ma, *Phys. Rev. Lett.* **102**, 160402 (2009).
 - [30] G. Zürn, F. Serwane, T. Lompe, A. N. Wenz, M. G. Ries, J. E. Bohn, and S. Jochim, *Phys. Rev. Lett.* **108**, 075303 (2012).
 - [31] J.-J. Wang, W. Li, S. Chen, G. Xianlong, M. Rontani, and M. Polini, *Phys. Rev. B* (2012) to be published.
 - [32] E. H. Lieb and F. Y. Wu, *Phys. Rev. Lett.* **20**, 1445 (1968).
 - [33] U. Busch and K. A. Penson, *Phys. Rev. B* **36**, 9271 (1987).